EXTENDED ESSAY

- PHYSICS -

The effect of blade diameter on wind turbine efficiency

How does varying the length of wind turbine blades impact their efficiency in generating electricity under consistent wind speeds?

Word Count: 3992

Table of Contents

1. INTRODUCTION

At 12 years old, I built my first ever wind turbine. We were having a sleepover with my best friend when she brought us a flower on a long stick. It would spin faster and faster every time we blew on it. After being mesmerized by all the colors mixing with each other, we decided to make personalized ones for ourselves. Following a bunch of tutorials online, we finally had ourselves new wind turbines. However, there was a problem. Mine was spinning way faster than hers. We tossed and turned the turbines around to catch their difference, which we later found that the reason was the fact that mine had slightly shorter blades.

After learning about aerodynamics and energy concepts in my IB Physics courses; I realized that the faster my wind turbine moved, the more energy it stored. I realized that times have changed, and renewable energy sources are becoming more and more demanded. Wind turbines have become one of the most promising energy sources of the future contributing to more than 10% of the total electricity production in the USA[1] (2022). Hence, I have decided dedicating my Extended Essay to explore to which blade lengths effect the efficiency and output of wind turbines. This research will allow me to gain deeper insight on aerodynamics, electromagnetic induction, renewable energy, and sustainable structures.

To conduct this experiment, a hand-made wind turbine model will be utilized. Since wind turbines are massive structures that are not allowed for personal use, as well as wind turbine kits being prone to give rise to systemic and random errors, 3D printed models combined with different equipment will be the optimal way of going through with the complex and involved situations that determine the efficiency of a small-scale wind turbine.

1. "Energy Fundamentals." *University of Leipzig*, home.uni-leipzig.de/energy/energy-fundamentals/15.htm. Accessed 9 Feb. 2023.

2. BACKGROUND INFORMATION

2.1 One-dimensional Momentum Theory & Betz Limit

Even if the flow through a wind turbine is highly complex due to the interaction between the rotor blades and the tip and root vortices, it is feasible to simplify the mechanisms. One-dimensional momentum theory can demonstrate that a few assumptions made regarding the rotors can simplify the analysis of a wind turbine. The theory assumes that the only flow through the turbine is across the "actuator disk" (*Figure 1*). The blades of the turbine – assumed to be an "actuator disk"- are inferred to be an infinitely thin permeable surface that is normal to the freestream direction and on which the wind flow is subjected to an equitable distribution of blade forces. According to the theory, the wind flow must be both steady (constant over time) and inviscid (free of viscous effects). Despite the chaotic and viscous nature of real-world wind flows, this reduction makes the mathematical model easier to handle. Furthermore, it is necessary to assume that the axial and tangential velocities are equally distributed throughout the actuator disk. This indicates that the forces are distributed across the annular space rather than centered on the blades.

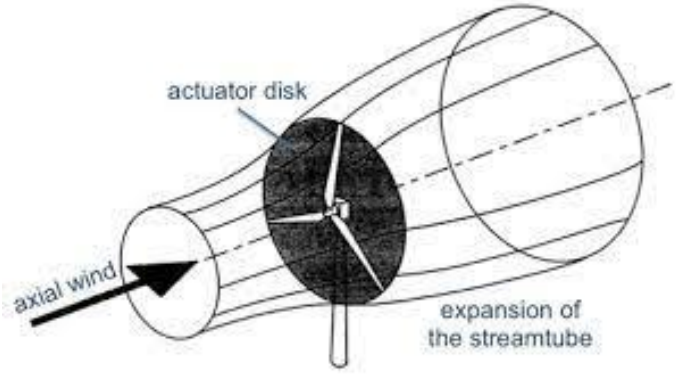

Figure 1: Actuator Disk Concept[2]

2.2 Swept Area

The rotor blades' circular path as they rotate is referred to as the wind turbine's swept area. It is the entire region that is swept through the air by the moving blades. The amount of wind energy that a wind turbine can catch and transform into mechanical and electrical power depends directly on this area.

$$A = \pi r^2$$

(Equation 1: swept area)

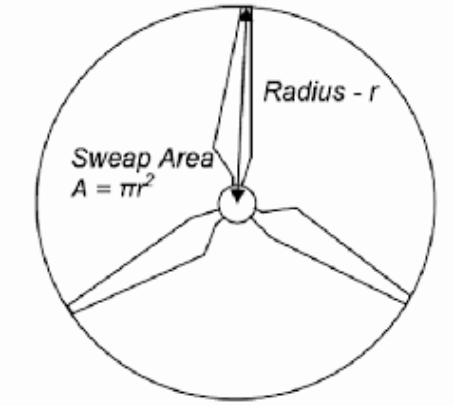

Figure 2: Swept Area of Rotor Blades[3]

Where:

- A is the swept area. (m^2)
- R is the radius of the rotor. (m)

Practically, the swept area is frequently calculated using the rotor diameter (the distance between one blade tip and the opposite blade tip), which is more easily understood and physically quantifiable.

A wind turbine's swept area is of utmost significance. It acts as a key factor of a wind turbine's ability to extract energy and, consequently, of its capability to generate power. It is crucial to maximize the capture of this energy since the kinetic energy carried by the wind is directly proportional to the cube of the wind speed. Greater wind energy inflow into the rotor because of a bigger swept area, increases the production of mechanical power.

3. Ghenai, Chaouki & Sargsyan, Nevzat. (2010). Wind Energy. 10.5772/13394.

2.3 Tip Speed Ratio

The tip speed ratio is a dimensionless parameter used to analyze and optimize the performance of a wind turbine rotor. The ratio between the tangential speed of a blade tip and the wind's actual speed, V, is known as the tip-speed ratio – λ or TSR – for wind turbines. Larger centrifugal forces at greater tip speeds necessitate stronger blades and increase noise levels.

$$\lambda = \frac{\omega \times R}{V}$$

(Equation 2: TSR)

Where;

- λ is the tip speed ratio
- ω is the angular velocity of the wind turbine blades, in rps
- R is the radius of the blades, in m
- V is the wind speed, in ms^{-1}

The power coefficient, represented as C_p, is a numerical value that indicates the percentage of wind energy that the wind turbine is harvesting. It is typically believed to depend on the pitch angle as well as the tip speed ratio. For instance, if a wind turbine produces power at a rate of 68.6% of the Betz Limit, its C_p would be 0.686 x 0.593 = 0.407. Therefore, 41% of the wind energy available is converted into electricity by this wind turbine.

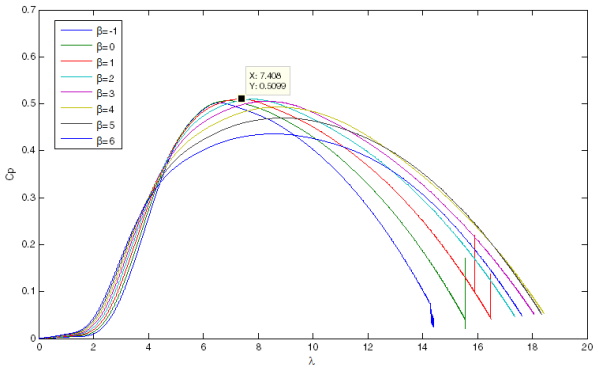

Figure 3: Relationship between TSR and C_p[4]

4. "cp_L_B.png ." NREL Forum, May 2017, forums.nrel.gov/t/windpack-1-5mw-power-coefficient/1596/5.

2.4 Wind Power Equation

In one second, the mass of air which flows past the turbine is ρA; where ρ is the density of air and A is the swept area of the turbine rotor. A can further be expanded by considering that the blade radius is r; so, A becomes πr^2. Where; V is the speed of air that enters the turbine, the wind energy entering the turbine is:

$$\frac{1}{2} \times m_{air} \times V^2 = \frac{1}{2} \times \rho V A \times V^2$$

$$= \frac{1}{2} \times \rho \times \pi r^2 \times V^3$$

Given the many assumptions made in the proof, the wind power equation gives the highest theoretical value of the available power. If the power coefficient (C_p) of a wind turbine were to be 1, this equation would be completely reliable. The equation can be altered to include the coefficient, and therefore becomes:

$$P = \frac{1}{2} \times \rho \times \pi r^2 \times V^3 \times C_p$$

(Equation 3: wind power)

2.5 Moment of Inertia

In rotational dynamics, the moment of inertia of a rigid body is defined as its resistance to rotational acceleration. It determines the quantity of torque required to accelerate a mass in the rotational axis. The general formula for the moment of inertia is:

$$I = \sum m_i r_i^2$$

Equation 4: moment of inertia

5. . Xia, Yuanye et al. "Wind Turbine Power Coefficient Analysis of a New Maximum Power Point Tracking Technique." *IEEE Transactions on Industrial Electronics* 60 (2013): 1122-1132.

2.6 Bernoulli's Principle

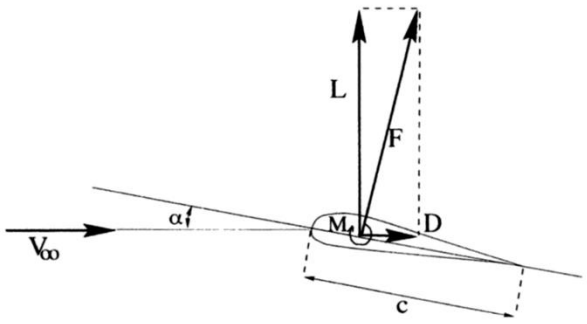

Figure 4: Lift and Drag Forces[5]

The principle states that a non-stationary fluid's speed is inversely proportional to the pressure it experiences and its potential energy. Hence, when the speed increases, the pressure is expected to decrease. In the case of wind turbines, when wind flows through the blades of the turbine, it decreases the pressure surrounding the rotors. The difference in pressure causes the air to move from high pressure to low pressure creating a lift force acting on the blades. This lift force results in the spin of the blades.

Where; m_i is the concentrated mass of the i^{th} component in the system and r_i is its center of mass' distance from the chosen axis. It can be observed that the moment of inertia of a system is directly proportional to its mass. Therefore, the greater the mass of the body, the larger amount of torque required to accelerate the system. The rotational kinetic energy of the body can also be calculated using its moment of inertia and its angular velocity. The equation is as follows; where ω is the angular speed.

$$\varepsilon = \frac{1}{2} I \omega^2$$

Equation 5: rotational kinetic energy

6. Hansen, Martin OL. *Aerodynamics of wind turbines: rotors, loads and structure*. Vol. 17. Earthscan, 2000.

3. HYPOTHESIS

According to the wind power equation, *Equation 3*, the power extracted from the wind by a wind turbine is directly proportional with the square of the radius of its blades. Therefore, an increase in energy extraction is expected to be observed with every increment in the diameter of the rotors. An increase in the power absorbed will allow more energy to be translated to electrical energy.

4. METHODOLOGY

4.1 Variables

Type	Variable	Controlling the Variable
Independent	Blade Diameter	The blade diameters were all set using technology (AutoCad).
Dependent	Efficiency	Measured using the same multimeter and anemometer on all trials.
Controlled	Wind Speed	Initial wind speed was set to a range between 6.47 – 6.55 ms^{-1}.
	Distances	All distances were kept constant and measured with a ruler.
	Motor	A StoreX 3V DC motor was utilized in all trials.

	Multimeter	The same Unit UT 136C+ Digital Multimeter was used in all trials.
	Anemometer	The same Unit UT 363 Anemometer was used in all trials.
	Wires	All copper wires had the same radius and length. They were all made from copper.

Table 1: Variables and Controlling the Variables

4.2 Materials

Material	Details
2 x HSF (heat sink and fan) fans	Fans should have dimensions between 92mm*x*92mm and 75mm*x*75mm.
2 x Plastic Stands	One stand with a height of 15cm, and the other with a height of 10cm.
5 x Blades	5 3D printed blades from PLA with their dimeters being 0.120m, 0.140m, 0.150m, 0.180m, 0.200m ($\pm\ 0.001m$).
5 x DC Motors	The motors used in this experiment are StoreX 3V DC Motors.
Ruler	A ruler that has 0.01m increments and a length of 0.30m ($\pm\ 0.01m$).

2 x Probe Wires	One wire for the anode and one wire for the cathode input of the multimeter.
10 x Copper Wires	Wires should all have the same dimensions. The wires employed in this experiment are all 7cm long.
2 x battery Clamps	-
Multimeter	The multimeter used for this experiment was Unit UT 136C+ Digital Multimeter.
Anemometer	The multimeter used for this experiment was Unit UT 363 Anemometer.
Electrical Tape	One roll of electrical tape should be sufficient.

Table 2: Materials

4.3 Set-up

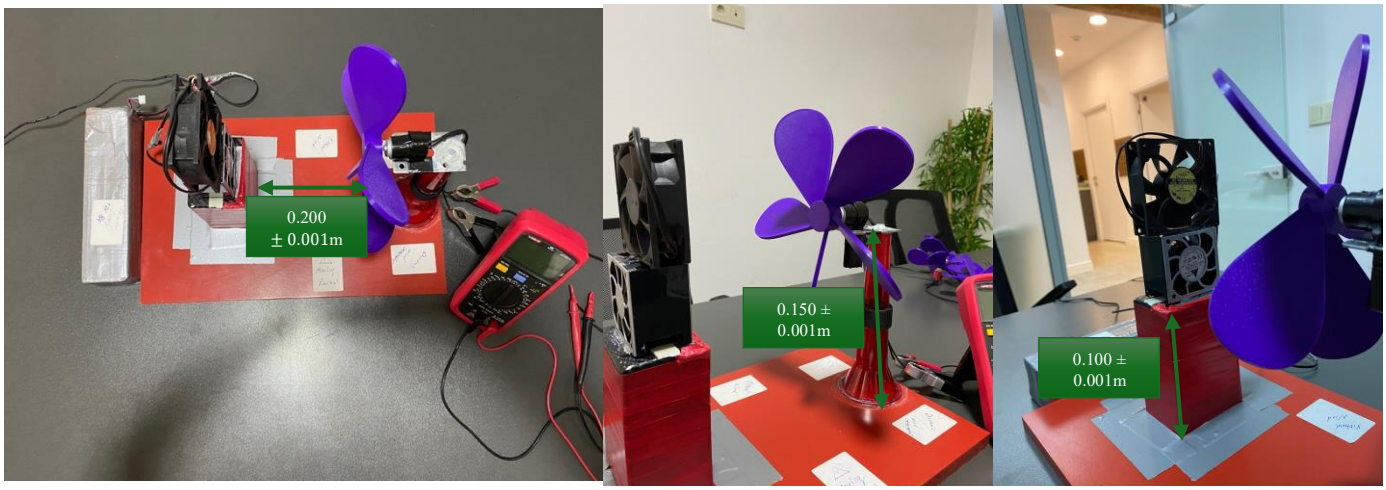

Figure 4,5,6: Apparatus of the Experiment

4.4 Procedure

I. Put the two plastic stands 0.200 ± 0.001m away from each other on a flat surface.

II. Attach a motor to the middle of each turbine.

III. Stick 2 fans on top of each other.

IV. Put the fans on top of the 0.10 ± 0.001m stand.

V. Connect the fans to the Lithium Polymer battery.

VI. Attach an on/off key to the turbines.

VII. Set up a camera facing the turbines side and start recording in slow-motion.

VIII. Put and secure the 0.12cm wind turbine to the 0.150 ± 0.001m stand.

IX. Attach one probe wire to the "COM" input of the multimeter. Attach the other probe wire to the "$V\Omega\mu AmA$℃" input of the multimeter.

X. Attach the 1 copper wire to the anode of the motor. Attach other clamp to the cathode of the motor.

XI. Use two battery clamps to connect the motor wires of the 0.12-meter turbine to the positive (+) and negative (-) parties of the multimeter.

XII. Start the fans.

XIII. Wait for 10 seconds and observe that the wind speed has averaged.

XIV. Bring the anemometer right between the fan and the turbine, with its center aligning with the center of the turbine.

XV. Start and record the average wind speed displayed by the anemometer for 30 seconds (V_1).

XVI. Bring the anemometer to the right rear cross of the turbine, with its center at the same height as the center of the turbine.

XVII. Start and record the average wind speed displayed by the anemometer for 30 seconds (V_2).

XVIII. Adjust the multimeter to display voltages between 0 to 4 volts; 3 digits after the comma.

XIX. Adjust the multimeter to display currents between 0 to 400 amperes; 3 significant figures after the comma.

XX. Set a 30 second timer.

XXI. Record the average values read off the multimeter for current and voltage during the timer.

XXII. Turn off the fans.

XXIII. Repeat the steps IV to XIV, 5 times.

XXIV. Repeat the steps III to XV for each wind turbine.

4.5 Risk Assessment & Ethical Considerations

In order to reduce the safety hazards that the motor and fan could pose since they utilize a DC current, careful and timely handling of them were considered. Other than the possible risk of electrical shock, no other hazardous situation was deemed important to overcome.

To take ethics into consideration, Polylactic Acid (PLA) is considerably the most biodegradable 3D printer filament to use. It is produced by extracting starch from renewable plant resources and manipulating them in a way to create thin and sturdy strips. The fan utilized in this experiment is also a second-hand one; so, all together they reduce the amount of waste produced.

5. DATA COLLECTION

5.1 Raw Data

Blade Diameter (m) $\pm$ 0.001	Trial #	Voltage (V) $\pm$ 0.001	Current (mA) $\pm$ 0.01	Final Wind Speed (ms^{-1}) $\pm$ 0.01	Period (s)$\pm$ 0.01
0.120	1	0.596	55.61	3.48	0.06
	2	0.585	56.03	3.45	0.06
	3	0.599	56.02	3.55	0.06
	4	0.594	55.03	3.49	0.06
	5	0.585	54.77	3.50	0.06
0.140	1	0.457	46.67	3.22	0.09
	2	0.460	47.15	3.20	0.09
	3	0.465	47.03	3.18	0.09
	4	0.463	46.67	3.25	0.09
	5	0.470	47.32	3.15	0.09
0.160	1	0.375	39.52	2.47	1.31
	2	0.373	38.96	2.55	1.31
	3	0.366	38.68	2.61	1.31
	4	0.362	38.13	2.57	1.31
	5	0.362	38.94	2.62	1.31
0.180	1	0.316	29.36	1.50	1.61
	2	0.315	29.43	1.53	1.61
	3	0.313	29.02	1.58	1.61
	4	0.312	29.08	1.45	1.61
	5	0.314	29.35	1.69	1.61
0.200	1	0.256	24.94	0.96	2.03
	2	0.263	25.06	0.94	2.03
	3	0.266	24.82	0.96	2.03
	4	0.260	24.78	1.16	2.03
	5	0.259	25.34	1.04	2.03

*The initial speed of the wind falls between the range of 6.47-6.55ms^{-1} in all trials.

Table 3: The Current, Voltage, Final Wind Speed and Period Values Recorded in the Investigation

6. DATA ANALYSIS

6.1 Processed Data

*All values displayed in the tables are average values of the trials.

Part A: Amount of Kinetic Energy Supplied by the Wind

$$\varepsilon = \frac{1}{2} \times 1.225 \times \pi r^2 \times \Delta {V_1}^3 \times \Delta t$$

Sample calculation for blade diameter 0.12 meters:

$\frac{1}{2} \times 1.225 \times 0.06^2 \times (6.55 - 3.47)^3 \times \pi \times 30$

$= 6.809$ J

(The following values are presented further in **Table 3**.)

Uncertainty Calculations:

The uncertainty will be calculated using the equation:

$$\frac{\Delta R}{R} + \frac{\Delta V}{V} + \frac{\Delta t}{t} = \Delta \varepsilon$$

Sample calculation for blade diameter 0.12m:

$$\frac{0.001}{0.12} + \frac{0.08}{3.08} + \frac{0.1}{30} = 0.0376$$

- 0.12m: $\pm 3.76 \times 10^{-2}$
- 0.14m: $\pm 3.51 \times 10^{-2}$
- 0.16m: $\pm 2.94 \times 10^{-2}$
- 0.18m: $\pm 2.49 \times 10^{-2}$
- 0.20m: $\pm 2.29 \times 10^{-2}$

A. The energy that the wind provides is purely kinetic since all measurements were taken from the same height. Multiplying *Equation 3* with Δt (30 seconds) will give the energy supplied by the wind.

Blade Diameter $\pm$ 0.001 (m)	Kinetic Energy Input (J)
0.120	$6.809 \pm 3.76 \times 10^{-2}$
0.140	$11.117 \pm 3.51 \times 10^{-2}$
0.160	$22.528 \pm 2.94 \times 10^{-2}$
0.180	$56.712 \pm 2.49 \times 10^{-2}$
0.200	$95.415 \pm 2.29 \times 10^{-2}$

Table 4: Kinetic Energy Input with Respective Blade Diameter

Part B: Center of Mass of Blades

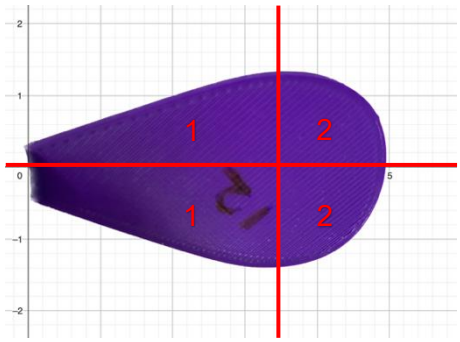

Figure 7: Blade Structure on a Cartesian Plane

The abscissa of their intersection point (*R)* will provide the distance of the center of mass from the center of the rotors. The perpendicular distance is the distance that creates the moment of inertia. Hence, $\frac{R}{\cos(30°)} - 30°$ as the flap angle of the blades – will be the accepted as the interspace that creates the torque. This distance (*r*) will be used in *Equation 4* and *Equation 5*.

(The following values are presented further in **Table 4.**)

B. Since the shape of the blade is an obovate, the center of mass should be further from the origin, when it the blade is fit into a cartesian plane. Therefore, the areas labelled 1 and 2 should be equal to each other. The outline of area 1 follows a parabolic pattern; whereas the outline of area 2 follows a circle. Solving the fitted lines for both areas simultaneously will provide the intersection point.

Blade Diameter $\pm$ 0.001 (m)	$r \pm 10^{-2}$ (cm)	Mass $\pm 10^{-2}$ (g)
0.120	4.53	0.704
0.140	5.33	0.829
0.160	6.49	0.959
0.180	7.64	1.144
0.200	8.79	1.346

Table 5: r Value and Mass of Each Blade Diameter

Part C: Moment of Inertia

Sample calculation for blade diameter 0.12m:

$$I = 8.71 + \sum_{1}^{5} \left(\frac{6.904 \times 10^{-3}}{9.81} \right) \times 4.53^2$$

$$I = 8.77\ kgm^2$$

(The following values are presented further in **Table 5**.)

Uncertainty Calculations:

The uncertainty will be calculated using the equation:

$$\frac{\Delta r}{r} \times 2 + \frac{\Delta m}{m} = \Delta MI$$

Sample calculation for blade diameter 0.12m:

C. The moment of inertia of each turbine differs due to their increase in both mass and radius. The values for *r* found in Part B, and the masses of the turbines measured by precision scales will be used in order to obtain their moment of inertia with *Equation 4.* With the same equation, the moment of inertia of the motor was calculated to be 8.71kgm^2, which will be added to the total moment of inertia of the systems.

$$\frac{0.002}{4.53} + \frac{0.001}{0.704} = 0.00186$$

- 0.120m: $\pm 1.86 \times 10^{-3}$
- 0.140m: $\pm 1.58 \times 10^{-3}$
- 0.160m: $\pm 1.35 \times 10^{-3}$
- 0.180m: $\pm 1.14 \times 10^{-3}$
- 0.200m: $\pm 0.97 \times 10^{-3}$

Blade Diameter $\pm$ 0.001 (m)	**Moment of Inertia (kgm^2)**
0.120	$8.77 \pm 1.86 \times 10^{-3}$
0.140	$8.77 \pm 1.58 \times 10^{-3}$
0.160	$8.77 \pm 1.35 \times 10^{-3}$
0.180	$8.77 \pm 1.14 \times 10^{-3}$
0.200	$8.77 \pm 0.97 \times 10^{-3}$

Table 6: Moment of Inertia with Respective Blade Diameter

Part D: Rotational Kinetic Energy

Sample calculation for blade diameter 0.12m:

$$\omega = \frac{2\pi}{0.06} = 104.7$$

$$\varepsilon = \frac{1}{2} \times 8.77 \times 10^{-4} \times 104.7^2$$

$\varepsilon = 5.56$ J

(The following values are presented further in **Table 6**.)

D. In order to use *Equation* 5, the angular velocity of each turbine should be obtained first. The equation for the angular velocity is $\omega = \frac{2\pi}{T}$; where T is the period of rotation. The period of rotation was measured using a slow-motion recording of the turbines.

Uncertainty Calculations:

The uncertainty will be calculated using the equation:

$$\frac{\Delta w}{w} \times 2 + \frac{\Delta I}{I} = \Delta \varepsilon$$

Sample calculation for blade diameter 0.12m:

$$\frac{0.02}{104.7} + \frac{0.00186}{8.77} = 4.03 \times 10^{-4}$$

- 0.120m: $\pm 4.03 \times 10^{-4}$
- 0.140m: $\pm 4.66 \times 10^{-4}$
- 0.160m: $\pm 4.32 \times 10^{-3}$
- 0.180m: $\pm 5.25 \times 10^{-3}$
- 0.200m: $\pm 6.56 \times 10^{-3}$

Blade Diameter $\pm$ 0.001 (m)	**Angular Velocity ($rads^{-1}$)**	**Rotational Kinetic Energy (J)**
0.120	$104.7 \pm 1.91 \times 10^{-4}$	$5.56 \pm 4.03 \times 10^{-4}$
0.140	$69.7 \pm 2.86 \times 10^{-4}$	$2.15 \pm 4.66 \times 10^{-4}$
0.160	$4.8 \pm 4.17 \times 10^{-3}$	$0.011 \pm 4.32 \times 10^{-3}$
0.180	$3.9 \pm 5.13 \times 10^{-3}$	$0.007 \pm 5.25 \times 10^{-3}$
0.200	$3.1 \pm 6.45 \times 10^{-3}$	$0.005 \pm 6.56 \times 10^{-3}$

Table 7: Rotational Kinetic Energy and Angular Velocity with Respective Blade Diameter

Part F: Electrical Energy Generated

$$\varepsilon = I \times V \times \Delta t$$

Sample calculation for blade diameter 0.12m:

$\varepsilon = 51.46 \times 10^{-3} \times 0.5118 \times 30$

$\varepsilon = 0.795\, J$

(The following values are presented further in **Table 7**.)

Uncertainty Calculations:

The uncertainty will be calculated using the equation:

$$\frac{\Delta I}{I} + \frac{\Delta V}{V} + \frac{\Delta t}{t} = \Delta\varepsilon$$

Sample calculation for blade diameter 0.12m:

$$\frac{0.01}{55.66} + \frac{0.001}{0.596} + \frac{0.1}{30} = 0.00519$$

- 0.120m: $\pm 5.19 \times 10^{-3}$
- 0.140m: $\pm 5.74 \times 10^{-3}$
- 0.160m: $\pm 6.27 \times 10^{-3}$
- 0.180m: $\pm 6.84 \times 10^{-3}$
- 0.200m: $\pm 7.54 \times 10^{-3}$

Blade Diameter $\pm$ 0.001 (m)	Electrical Energy (J)
0.120	$0.795 \pm 5.19 \times 10^{-3}$
0.140	$0.652 \pm 5.74 \times 10^{-3}$
0.16	$0.428 \pm 6.27 \times 10^{-3}$
0.180	$0.275 \pm 6.84 \times 10^{-3}$
0.200	$0.195 \pm 7.54 \times 10^{-3}$

Table 8: Electrical Energy with Respective Blade Diameter

Part G: Efficiency

Sample calculation for blade diameter 0.12m:

6.809 – 5.563 = 1.246

$$\frac{0.795}{1.246} \times 100 = 64.9\%$$

(The following values are presented further in **Table 8**.)

Uncertainty Calculations:

The uncertainty will be calculated using the equation:

$$\frac{\Delta\varepsilon_{electric}}{\varepsilon_{electric}} + \frac{\Delta(\varepsilon_{wind} - \varepsilon_{rotation})}{(\varepsilon_{wind} - \varepsilon_{rotation})} = \Delta Efficiency$$

Sample calculation for blade diameter 0.12m:

$$\frac{0.00520}{0.795} + \frac{0.0380}{1.249} = 0.0370$$

G. The efficiency of the turbines will be calculated in the form of percentages. First, the remaining energy from the loss to rotational kinetics will be calculated. Then, the electrical energy will be proportioned to the remaining energy.

- 0.120m: $\pm 3.70 \times 10^{-2}$
- 0.140m: $\pm 1.28 \times 10^{-2}$
- 0.160m: $\pm 1.61 \times 10^{-2}$
- 0.180m: $\pm 2.54 \times 10^{-2}$
- 0.200m: $\pm 3.87 \times 10^{-2}$

Blade Diameter $\pm$ 0.001 (m)	**Efficiency (%)**
0.120	$64.781 \pm 3.70 \times 10^{-2}$
0.140	$7.268 \pm 1.28 \times 10^{-2}$
0.160	$1.900 \pm 1.61 \times 10^{-2}$
0.180	$0.485 \pm 2.54 \times 10^{-2}$
0.200	$0.205 \pm 3.87 \times 10^{-2}$

Table 9: Efficiency with Respective Blade Diameter

6.2 Graphs

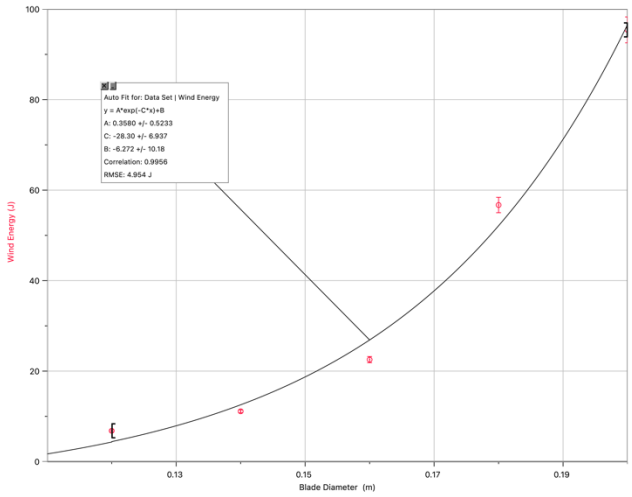

Graph 1:Blade Diameter against Wind Energy

Equation: $0.358e^{-28.3R}$- 6.272

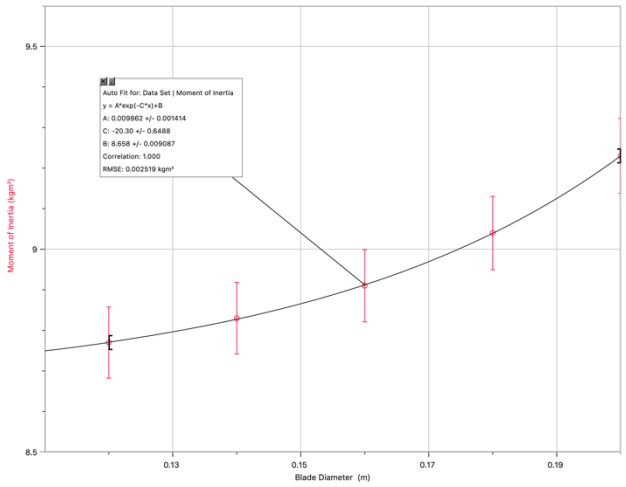

Graph 2:Blade Diameter against Moment of Inertia

Equation: $0.009862e^{-20.3R}$- 8.6

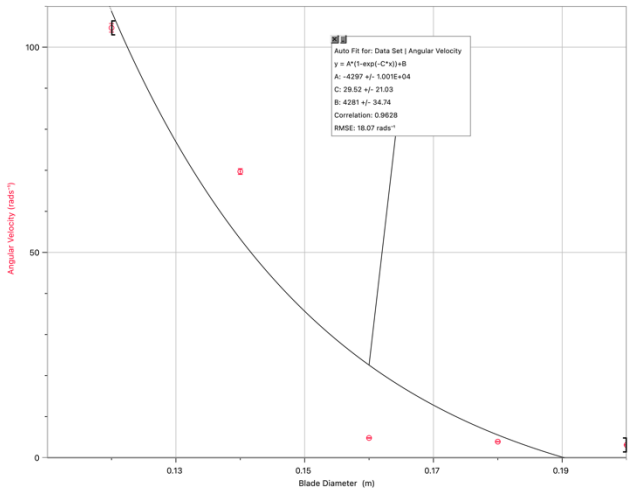

Graph 3:Blade Diameter against Angular Velocity

Equation: -4297(1-$e^{-29.52R}$)- 4281

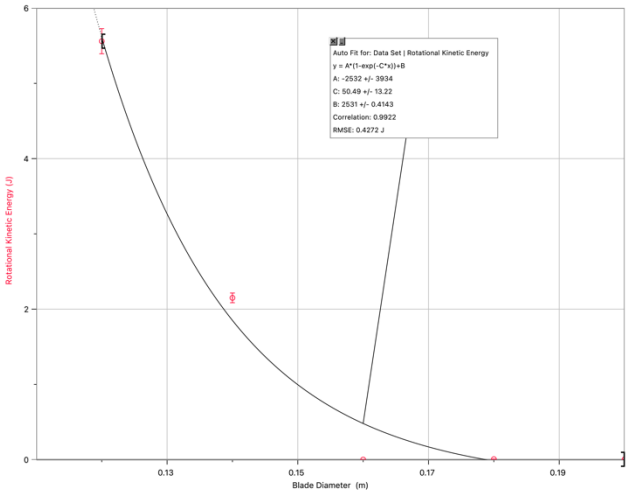

Graph 4:Blade Diameter against Rotational Kinetic Energy

Equation: -2532(1-$e^{-50.49R}$)- 2531

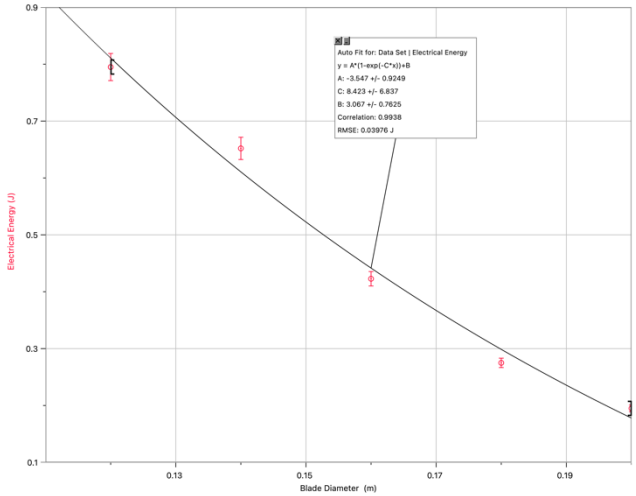

Graph 5:Blade Diameter against Electrical Energy

Equation: -3.547(1- $e^{-8.423R}$)+ 3.067

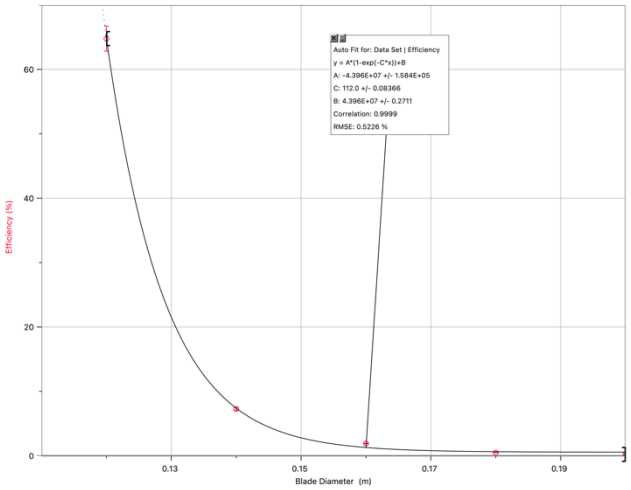

Graph 6:Blade Diameter against Efficiency

Equation: -4.396(1- e^{-112R}) + 4.396

6.3 Linearization

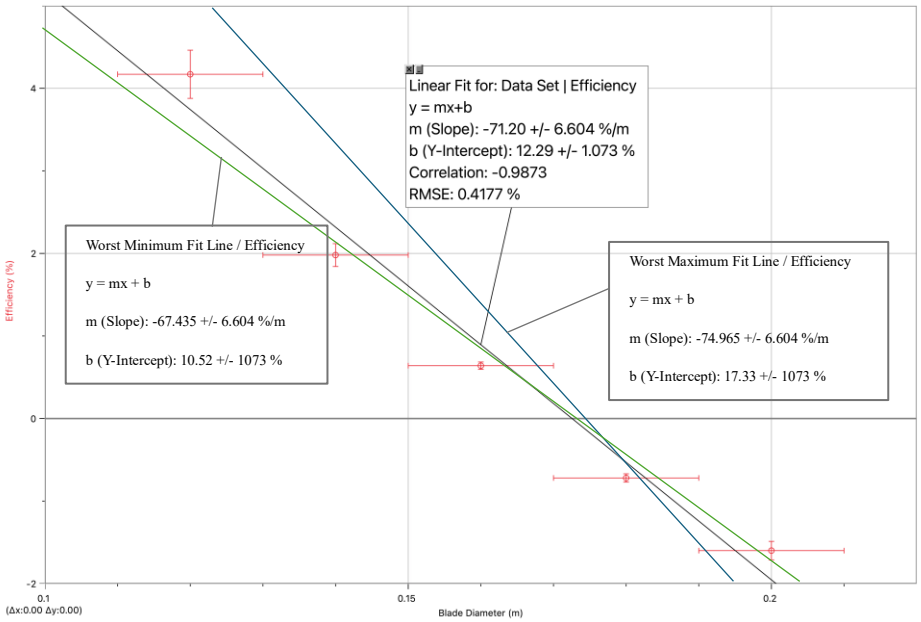

Graph 7: Linearization of Graph 6

Equation: -71.2R + 12.29

<u>Error Propagation:</u>

The uncertainty of the results is found using the equation:

$$\frac{|m_{max} - m_{min}|}{2} = |\delta|$$

$$\frac{74.965 - 67.435}{2} = 3.765$$

Hence; the uncertainty of the results is 3.765.

7. CONCLUSION & EVALUATION

Interpreting Data

The research question "How does varying the length of wind turbine blades impact their efficiency in generating electricity under consistent wind speeds?" and; hence, the ability of a small-scale wind turbine connected to a motor in converting mechanical energy to electrical energy can be directly observed from *Graph 6*. The graph of efficiency against blade diameter displays an exponential decay. When plotted against each other, the best fit line occurs to be a base e exponential. This shows an inverse proportional relationship between the variables. Thus, the hypothesis of a quadratic growth with respect to blade diameter was disproved. The results varied from the data obtained from existing literature due to the fact that in real-life turbines, an AC motor is occupied to generate electricity. Nevertheless, in small-scale experimentations such as this, an AC motor would be almost impossible to employ considering their size. The usage of a DC motor; therefore, deviated the obtained data from existing data. There are also a few different explanations for the deviation from the hypothesis.

7.1 Increase in Rotational Kinetic Energy

The moment of inertia of a rotating object was expected to increase prior to the experiment. As observed in *Graph 2*, the moment of inertia grows exponentially as the blade diameter increases. The increase in inertia will cause the turbines to resist to the lift force that is the main source which drives the rotation of the turbines. The same quantity of wind is provided to each turbine; therefore, the fans are limited with the amount of lift force they supply. The combination with the constraint in lift force and the increasing moment of inertia will eventually lead to the turbines starting to rotate less effectually with each increment in blade diameter.

As the diameter increases, we can observe a decrease in angular velocity. This instance is attributed to the fact that the angular distance covered is not dependent on the blade diameter. Nevertheless, the time taken to cover that distance (2π) will become larger with the increase in diameter. The period of rotation will increase since-as mentioned previously-the amount of lift force, hence also the angular acceleration, decreases gradually when blade diameter increases. Thus, when the acceleration is reduced the angular velocity will also decrease. The angular velocity of the turbines has a direct effect on the angular velocity of the motor. If the turbines slow down, the motor will proportionally reduce in velocity, resulting in decreased electrical energy generation.

According to *Equation 5*, square of the angular velocity is directly proportional with the kinetic energy required for rotation. Even though the moment of inertia increases, the angular velocity decreases by a larger factor. Consequently, the rotational kinetic energy exhausted by the turbines decrease with the increases in blade diameter.

7.2 Profile Drag

One type of drag force is the profile drag; which is the force that arises from the friction between the surface of the turbine blades and the air molecules surrounding it. As foreseen, the quantity of profile drag is directly proportional with the blade diameter. This relationship is strictly linear. The value of profile drag forces acting on the same unit area of the blades are all equal; hence, as surface area increases the total profile drag acting on a blade will add up since the net force acting on a system is the vectoral sum of all individual forces.

7.3 Wake Interference & Turbulence (Boundary Layer Effects)

The experimental system-containing all of the components- spans across a 30cm×11cm area. The fans are all approximately 23cm away from the turbines. This is a relatively short distance, potentially explaining the decaying trendline. A compact system such as this will allow the boundary layer effects to be more resolute than a larger framework.

The wake effect, as in the disturbed air flow around the turbines, is a significant factor that alters the data. Wake effect is produced when the wind entering the cover ground of a wind turbine is scattered around the turbine with a different final velocity. This effect will be substantially greater in blades with larger diameters. As blade diameter increases, the force of impact experienced by the air molecules that get in contact with the system also increases. This produces a turbulent flow around the turbine. As impact intensifies, the difference between the final and initial velocity will gradually amplify as well. Different velocities of wind will produce different pressures around them; and the pressure of fluid molecules are inversely proportional with their velocity (*2.4 Bernoulli's Principle)*. The greater the difference in pressure; the greater wake interference that will be fabricated. The wake interference pattern created by the difference in pressure will counteract the lift force which rotates the turbines. The force that is responsible for this effect is induced drag. The quantity of induced drag will add up as blade diameter increases; thus, the rotation of the turbines will be hindered.

7.4 Tip Speed Ratio

The tip to speed ratio plays a vital role in the efficiency of wind turbines. The TSR is inversely proportional with blade length, observed in *Table 9.1*. At lower TSR values, the angle of attack of the blades relative to the wind may be suboptimal, resulting in decreased lift and increased drag.

This can reduce the overall efficiency of the turbine in converting wind energy into rotational motion. Additionally, operating at lower TSR values can increase turbulence and stress on the turbine blades. This can lead to higher mechanical loads and fatigue, also reducing the efficiency of the system.

Evaluation

7.5 Strengths

Wide Blade

Before choosing this model that resembles flower petals for the blades, a NREL-5MW HWAT 3-blade system was selected. However, since the NREL blades are very thin and permeable to wind, they could not absorb enough energy from the wind to rotate and produce electrical currents. Hence, choosing a wider blade allowed for a higher ratio of wind power to be extracted since it did not allow wind to pass through as easy as the NREL blades. Despite the fact that the center of mass of the blade was slid further away from the gearbox increasing its moment of inertia, choosing a thinner blade would be completely unusable for the sake of this exploration.

Power Loss due to Friction

The material used to print the blades are Polylactic Acid (PLA). The coefficient of friction of PLA typically ranges from 0.15 to 0.28. This range is far less than most other plastics used for 3D printing, such as coated ABS which is a filament with a coefficient of friction reaching 0.80 at times. A low coefficient of friction means that the amount of work done against friction will be less. This can be effective in utilizing all the power gained from the nonstationary wind. It reduces the torque required the turn the system while reducing the energy consumed to overcome friction.

DC Motor

Existing literature states that DC motors tend to be far more efficient in small-scale systems with low wind speeds. Field excitation is one of the reasons. In DC motors, the magnetic field that drives the induction of electricity is generated by either a permanent magnet or an electromagnet. Both of these produce a relatively constant magnetic field. The speed at which the motors are spinning is also on the lower side owing to the meager wind speeds. These two factors combined together will forge the field excitation-change in magnetic field- to remain relatively constant, resulting in consistent motor performance.

7.6 Weaknesses

Uniform Wind

While using uniform wind in wind turbine simulations is often necessary for simplification, it has significant drawbacks as compared to more realistic simulations that incorporate varied wind conditions into account.

They lack realism since they fail to effectively simulate real-world wind conditions to which wind turbines must react. This oversimplification not only compromises the underlying complexity of wind dynamics, but also results faulty predictions. Uniform wind simulations do not capture this variance well, which can lead to inaccurate data, especially in places with varying wind patterns.

Because of the limitations in the production of this research, uniform wind simulation was the only path to consider obtaining the explorative data. Nevertheless, more in-depth, and accurate experimentation should include realistic and ranging wind conditions when evaluating the efficiency of wind turbines.

Change in Mass

The mass of the blade has unavoidably increased proportionally with each increment in blade diameter. As mentioned in *2.5 Moment of Inertia*, the masses of the blades have a huge impact on their moment of inertia. An increase in mass results in an increase in its inertia. More inertia means more power required to accelerate the system; therefore, as blade diameter increases, the amount of power essential to be extracted from the wind should increase also. s

A fluctuation in mass will only be prominent in larger wind turbines since mass is directly proportional to volume. Two realistically scaled 60.0 m and 61.0 m blades will have a greater difference in mass than two blades of length 0.12 m and 0.14 m. It can, accordingly, be deemed unnecessary to address the shift in the mass of the blades in the context of this experiment.

It would also be impossible to keep the mass constant without changing any other variable than blade diameter. To produce a consistent mass while adjusting the blade radius, numerous important elements of the blade must be changed, including its material, thickness, and perhaps other structural aspects. Making these changes to the blade's composition and form would inject a slew of new independent variables into the simulation, which might have a substantial impact on the results. As a result, to keep the study scope manageable and focused, the decision was made to vary the blade radius while allowing the mass to shift naturally.

Scale of Wind

On average and non-extreme conditions, real-life wind turbines are subjected to 8.5-10 m of wind per second. In this exploration, a wind speed of V_1 was exposed to the turbines. The proportion of wind speed to blade radius is far greater in the simulation data than in reality. This will unavoidably create a dilation in the power available to the turbines. Regardless of how, a

wind speed with a lower speed would not create enough difference in the power extracted by each turbine diameter to be analyzed. Hence, the velocity of the wind was chosen to be V_1, even though it surpasses the proportions.

Period of Rotation

As mentioned in *4.3 Procedure*, the turbines were recorded in slow-motion during the trials. The recordings were taken in order to obtain the period of rotation for each blade diameter. The period is required to calculate angular velocity; thus, the energy lost to rotational kinetic energy. Even though the camera used for this investigation can capture images at 240fps (frames per second), human eye is still responsible for the final reading. Hence, slight altercations may have occurred in the readings for the period of rotation. This can be regarded strictly as a random error. It can be prevented using more precise equipment with a higher *fps* count; such as a digital video camera. Nonetheless, since multiple trials were conducted, the effect of such error would be conspicuous and considered an outlier. All period of rotation values were supported by each other; therefore, it can be implied that little or no inaccuracy occurred for the measurements of time period.

8. APPENDIX

8.1 Tip Speed Ratio

Part X: Tip Speed Ratio

The tip speed ratio is calculated using *Equation 2.*

Sample equation for blade diameter 0.12m:

$$\lambda = \frac{104.7 \times 0.0585}{3.92 \times 10^{-2}}$$

$$\lambda = 156.25$$

(The following values are presented further in **Table 9.1**.)

Blade Diameter $\pm 10^{-4}$ (m)	TSR
0.120	62.9
0.140	49.7
0.160	4.15
0.180	4.0
0.200	3.6

Table 8.1: TSR with Respective Blade Diameter

8.2 Turbine Details

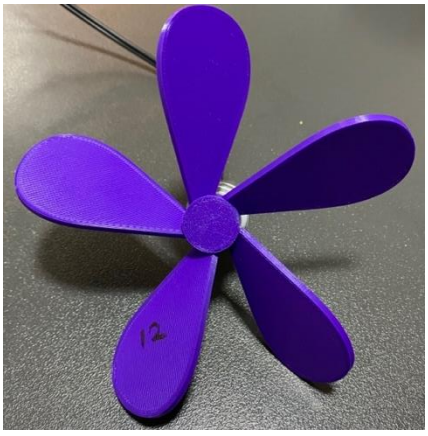

Figure 8.1: Close Up Image of Blade with Diameter 0.120m

The turbines were all scaled proportionally without making any arrangement regarding their horizontal width.

The mass is distributed uniformly throughout the turbines.

The radius of the center cylinder that encapsulates the motor was constant for all blades.

All turbines were printed with the same 3D printing machine.

8.3 Set-up Details

Figure 8.2: Battery Clamp Attachment

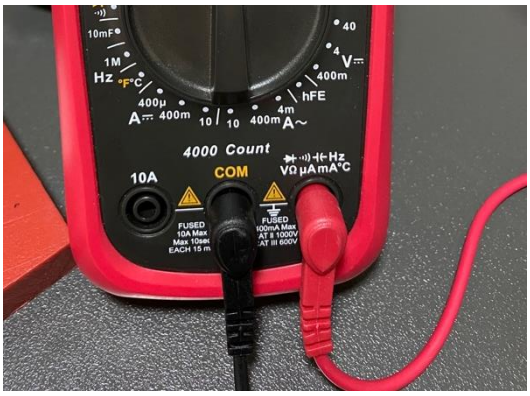

Figure 8.3: Multimeter Set-up

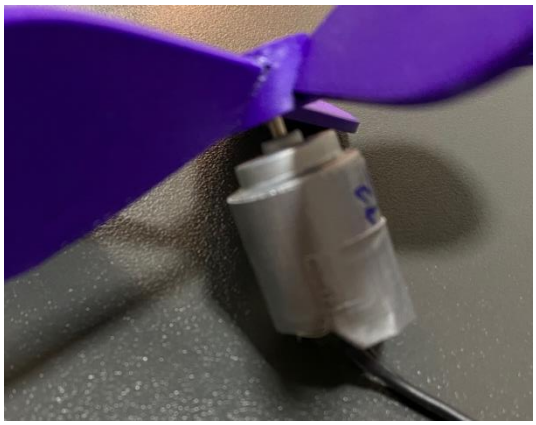

Figure 8.4: Motor and Turbine Connection

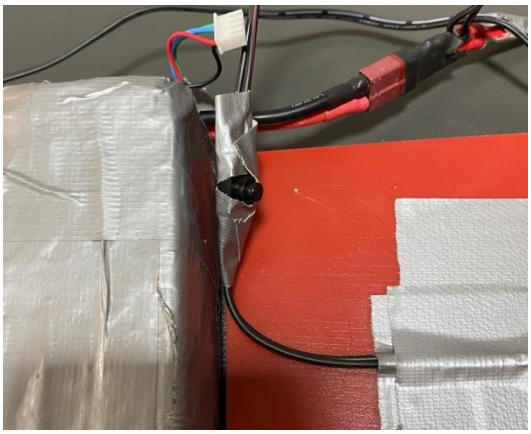

Figure 8.5: LiPo Battery and on/off Key Set-up

9. REFERENCES

Giebultowicz, Tom. "6.4: The Physics of a Wind Turbine." *Engineering LibreTexts*, eng.libretexts.org/Sandboxes/jhalpern/Energy_Alternatives/06%3A_Windpower/6.04%3A_The_Physics_of_a_Wind_Turbine. Accessed 9 Feb. 2023.

Grogg, Kira. "Harvesting the wind: the physics of wind turbines." *Physics and Astronomy Comps Papers* 7 (2005).

Douak, M., et al. "Wind energy systems: Analysis of the self-starting physics of vertical axis wind turbine." *Renewable and Sustainable Energy Reviews* 81 (2018): 1602-1610.

Cox, Kevin, and Andreas Echtermeyer. "Structural design and analysis of a 10MW wind turbine blade." *Energy Procedia* 24 (2012): 194-201.

Yang, Han, Jin Chen, and Xiaoping Pang. "Wind turbine optimization for minimum cost of energy in low wind speed areas considering blade length and hub height." *Applied Sciences* 8.7 (2018): 1202.

Pasupulati, Subbaiah V., Jack Wallace, and Mark Dawson. "Variable length blades wind turbine." *IEEE Power Engineering Society General Meeting, 2005*. IEEE, 2005.

Buckney, Neil, et al. "Structural efficiency of a wind turbine blade." *Thin-Walled Structures* 67 (2013): 144-154.

Sharma, R. N., and U. K. Madawala. "The concept of a smart wind turbine system." *Renewable energy* 39.1 (2012): 403-410.

Libii, Josué N., and David M. Drahozal. *The Influence of the Lengths of Turbine Blades on the Power Produced by Miniature Wind Turbines That Operate in Non-uniform Flow Fields*. 2nd ed., vol. 10, *World Transactions on Engineering and Technology Education*, 2012. pp. 1-6.

Parise, Tom. "Wind Turbine Design." *Stanford University*, 10 Dec. 2011, large.stanford.edu/courses/2011/ph240/parise1/. Accessed 10 Sept. 2023.

Wilson, R. E. "Wind-turbine aerodynamics." *Journal of Wind Engineering and Industrial Aerodynamics* 5.3-4 (1980): 357-372.

Wang, Tongguang. "A brief review on wind turbine aerodynamics." *Theoretical and Applied Mechanics Letters* 2.6 (2012): 062001.

Schaffarczyk, Alois Peter. *Introduction to wind turbine aerodynamics*. Springer Nature, 2020.

Ju, Beomcheol & Jeong, Jihyun & Ko, Kyungnam. (2016). *Assessment of Wind Atlas Analysis and Application Program and computational fluid dynamics estimates for power production on a Jeju Island wind farm*. Wind Engineering. 40. 10.1177/0309524X15624346.

Abe, K., Nishidab, M., Sakuraia, A., Ohyac, Y., Kiharaa, H., Wadad, E., Sato, K.: Experimental and numerical investigations of flow fields behind a small wind turbine with a flanged diffuser. J. Wind Eng. Ind. Aerodyn. 93, 951–970 (2005)

Glauert, H.: Airplane Propellers. Division L. In: Durand, W.F. (ed.) Aerodynamic Theory, vol. IV, pp. 169–360. Springer, Berlin (1935)

Coelho, Paulo. *The Betz Limit and the Corresponding Thermodynamic Limit*. 2nd ed., vol. 47, 202AD, https://doi.org/10.1177/0309524X221130109.

UBC Physics & Astronomy Outreach. “PRIVATE: Wind Turbines – Betz Law Explained.” *The University of British Columbia*, c21.phas.ubc.ca/article/wind-turbines-betz-law-explained. Accessed 6 Feb. 2024.

Yılmaz, Sinan. “Comparative Investigation of Mechanical, Tribological and Thermo-Mechanical Properties of Commonly Used 3D Printing Materials.” *European Journal of Science and Technology*, no. 32, Dec. 2021, pp. 827–31. https://doi.org/10.31590/ejosat.1040085.